This article has been accepted for publication in a future issue of this journal, but has not been fully edited. Content may change prior to final publication. Citation information: DOI 10.1109/TMECH.2021.3084311, IEEE/ASME Transactions on Mechatronics

Anthropomorphic Prosthetic Hand Inspired by Efficient Swing Mechanics for Sports Activities

Mun Hyeok Chang*, *Student Member, IEEE,* Dong Hyun Kim*, Sang-Hun Kim, *Student Member, IEEE,* Yechan Lee, Seongyun Cho, Hyung-Soon Park#, *Member, IEEE* and Kyu-Jin Cho#, *Fellow, IEEE*

***Abstract*—Swinging—generating high impact by maximizing the speed of motion—is essential in sports activities. However, designing prosthetic hands suitable for swinging is still a challenge. Herein, we propose a swing-dedicated prosthetic hand that adopts the anatomical features of humans for an efficient swing. Our design, inspired by the joint arthrokinematics and tendon routing of fingers, enables a diagonal power "squeeze" grip robust to impact while increasing the reach of the clubhead. The swing speed is further increased by radio/ulnar deviation of the wrist and its nonlinear stiffness change achieved by the passive clutch mechanism. We evaluated our prosthetic hand through golf and found that it sustained high impact with diagonal grip, and clubhead speed increased by 19% at 90 rpm, with the radio/ulnar deviation nonlinearly correlated with arm angle. Our prosthetic hand design will contribute to improving amputees' quality of life by allowing them to participate in sports activities.**

***Index Terms*—Hand prosthesis, robotic hand, bio-inspired design, swing mechanics, power-sqeeze grip, differential mechanism, sports device.**

I. Introduction

SINCE humans started using tools, "swinging," to impact a target with a club, has been used in vital areas of life. Swinging was used to hunt and create stone tools in ancient times, and in modern times it is used in various areas, such as hammering, fishing, and sports activities [1], [2]. To convey impact during a swing, holding the club diagonally is crucial for increasing leverage by aligning the club with the forearm [3], [4]. In order to stably hold the club diagonally at impact, the individual performs a power "squeeze" grip by using their fingers, palm, and thumb simultaneously (Fig. 1(a)), a unique function of the human hand [4], [5]. The arthrokinematics at the carpometacarpal (CMC) joints of the hand, consisting of flexion and supination, produces concavity of the palm allowing the fingers and the palm to simultaneously fit around the club for power squeeze grip [6]. Multiple flexion muscles of the human hand contract simultaneously to increase finger joint stiffness and produce secure grasping against external forces. The large range of motion (ROM) of the radio-ulnar deviation of the wrist and its coordination during swing also contribute to producing a powerful impact [3]. The radio-ulnar deviation of the wrist is produced by rolling and gliding among two-row carpal joints of the wrist. Humans reduce inertial resistance of the swinging by radially deviating the wrist during cocking phase, and instantaneously increase the reach length by the ulnar deviation of the wrist during swing phase to maximize the clubhead speed at impact (Fig. 1). Mimicking these biomechanics is important for effective swinging and particularly highly affects the performance of sports activities.

Sports activities improve quality of life for amputees by increasing their social contact and improving their motor skills

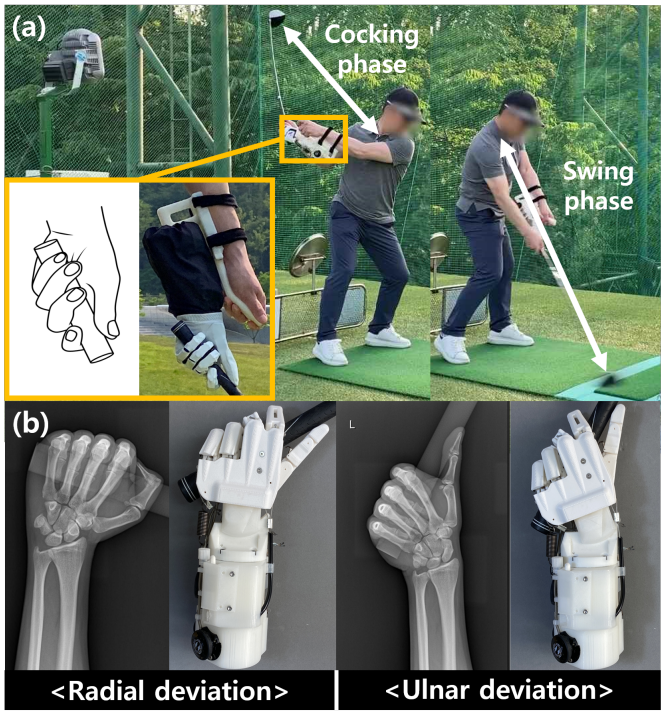

Fig. 1. **Anthropomorphic prosthetic hand inspired by efficient swing mechanics.** (a) Golf swinging by a non-amputee golfer wearing our prosthetic hand. The power squeeze grip of a human hand aligning the club and forearm with wrist deviation is achieved by the proposed prosthetic hand to maximize clubhead speed. For efficient swinging, our prosthetic hand produces radial deviation of the wrist in the cocking phase to reduce the reach length and inertial resistance of the swinging, and the ulnar deviation of the wrist in swing phase to align the club and forearm to maximize the clubhead speed. (b) The radio–ulnar deviation of the human wrist and the proposed prosthetic hand. X-ray images are provided by SNUBH.

This research was supported by the convergence technology development program for bionic arm through the National Research Foundation of Korea (NRF) funded by the Ministry of Science & ICT (NRF-2015M3C1B2052817). This work was supported by the Korea Medical Device Development Fund grant funded by the Korea government (the Ministry of Science and ICT, the Ministry of Trade, Industry and Energy, the Ministry of Health & Welfare, the Ministry of Food and Drug Safety) (Project Number: KMDF_PR_20200901_0175, 9991007396). This work was supported by the National Research Foundation of Korea(NRF) grant funded by the Korea government(MSIT) (No. 2020R1A2C2012641).

M. H. Chang, S.-H Kim, and K.-J Cho (corresponding author e-mail: kjcho@snu.ac.kr) are with School of Mechanical and Aerospace Engineering, Seoul National University, Gwanak-ro 1, Gwanak-gu, Seoul, Korea.

D. H. Kim, Y. Lee, S. Cho, and H.-S Park (corresponding author e-mail: hyungspark@kaist.ac.kr) are with Mechanical Engineering Department, Korea Advanced Institute of Science and Technology, Yuseong, Daejeon, Korea.

This article has been accepted for publication in a future issue of this journal, but has not been fully edited. Content may change prior to final publication. Citation information: DOI 10.1109/TMECH.2021.3084311, IEEE/ASME Transactions on Mechatronics

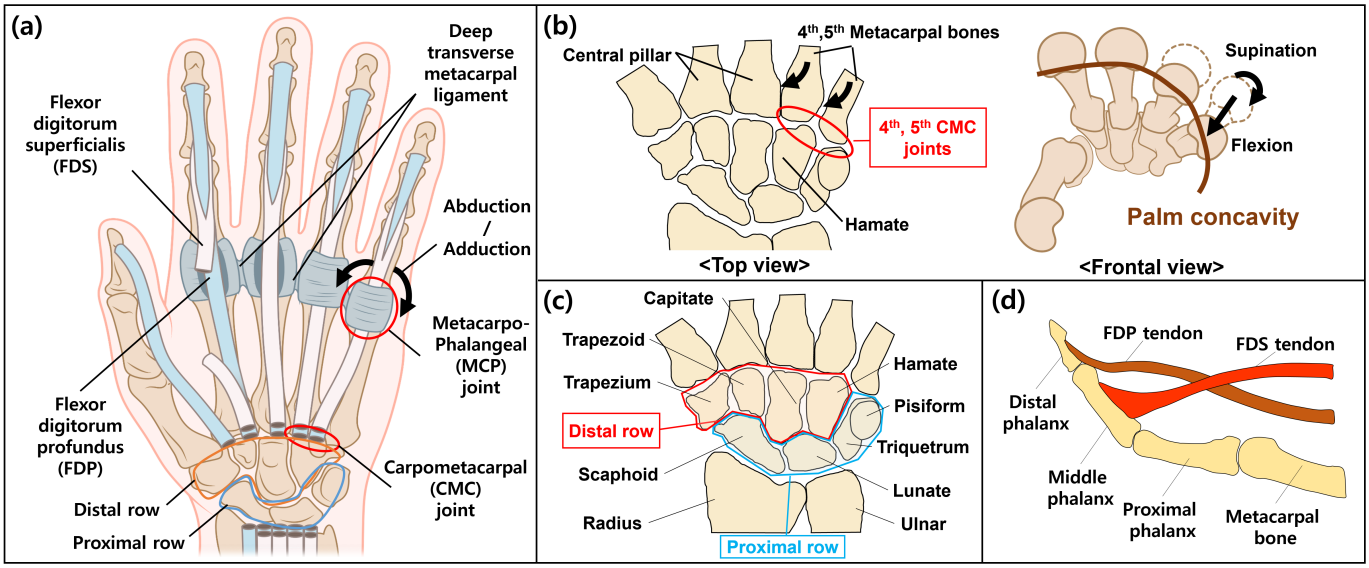

Fig. 2. **Anatomical features of the human hand for efficient swinging.** (a) Entire anatomical features of human hand and wrist. (b) Flexion coupled with supination of metacarpal bones produced by fourth and fifth CMC joints. (c) Anatomical structure of the carpal bone. The eight components of the bone are set in a two-rowed structure. The asymmetric structure enables the wrist to have larger ROM of ulnar deviation. (d) FDP and FDS tendon routing adopted to explore and design the tendon routing of the prosthetic hand.

and muscle strength [7]–[9]. Achieving high-speed swinging with an anthropomorphic prosthetic hand would allow amputees to engage in sports activities, e.g., golf, tennis, baseball, fishing, that involve swinging a club. However, the development of anthropomorphic hands has focused on achieving grasps for activities of daily living (ADLs), and designing anthropomorphic hands capable of high-speed swinging is a challenge in robotics [10]. To achieve grasps for ADLs, many anthropomorphic hands have adopted the structural features of human hands, such as bones, ligaments, transmissions [11]–[18], and human hand kinematic and kinetic characteristics [19]–[22] to exploit the high grasping performance. To reduce the weight and complexity of the prosthesis for usability, recently developed prostheses have used underactuation to actuate the fingers with a reduced number of actuators [23]–[27]. Although these hands have been shown to be capable of performing grasping movements in everyday life, physical activities that require high-speed swinging must still be addressed [28]. Unlike the required grip force of ADLs, which is approximately 45–68 N [29], [30], a power grip force could reach 400 N, exceeding the practical usability of current prosthetic hands [31]. Non-anthropomorphic prosthetic accessories dedicated to swinging have been developed to allow amputees to engage in physical activities [32], [33]. While these dedicated prosthetic accessories allow amputees to perform swinging, they have appearance limitations that greatly influence the use of prostheses [34].

In view of the current state of the art and identified knowledge gap, this paper presents the design of an anthropomorphic prosthetic hand dedicated to swinging that achieves the power squeeze grip and the phase change of the wrist for an efficient swinging by adopting the anatomic features of the human hand (Fig. 1). We adopt arthrokinematics enabled by the carpal bone structures (CMC joints and carpal joints) and the adjustability of the stiffness of the fingers and the wrist. The flexion and supination of the CMC joints are implemented with two-degree-of-freedom (2-DOF) joints actuated through 2-DOF under-actuated tendon routings, which allows fingers and palm to adapt to the club while holding the club diagonally. The two-rowed structure of the carpal bone of the wrist is replicated to produce radio-ulnar deviation with similar ROM of human wrist while keeping the design compact but robust to external force [35]. Multiple finger flexors were explored to reinforce the joint stiffness of fingers with respect to external forces, and a differential actuation system is implemented for tendon excursion with fewer actuators. The instantaneous change of radio-ulnar deviation movements induced by providing nonlinearity of effective wrist joint stiffness during the swing, enabled by implementing a clutch mechanism; maintaining high stiffness at the early phase, and dramatically reducing the stiffness near impact, at a certain point that can be adjusted. The performance of our prosthetic hand was evaluated through an impact test and golf swinging, which is one of the most challenging swinging examples because of its high speed and load. Our prosthetic hand will allow amputees to perform high-speed swinging efficiently and safely and will contribute to improving their quality of life by enabling them to engage in physical activities that require high-speed swinging.

The rest of this paper is organized as follows. Section II introduces the detailed anatomical features of human hand and wrist for efficient swing mechanics. The proposed hand and wrist designs are demonstrated in Section III and IV, respectively. The experimental results are presented in Section V. Discussion and conclusion are demonstrated in Sections VI.

II. Anatomical Features for Effective Swing

The anatomical features adopted to design the proposed prosthesis dedicated to swinging are shown in Fig. 2. For achieving an efficient swing, the club should be grasped diagonally to increase the reach length. The concavity of the palm mainly contributes to gripping the club diagonally.

This article has been accepted for publication in a future issue of this journal, but has not been fully edited. Content may change prior to final publication. Citation information: DOI 10.1109/TMECH.2021.3084311, IEEE/ASME Transactions on Mechatronics

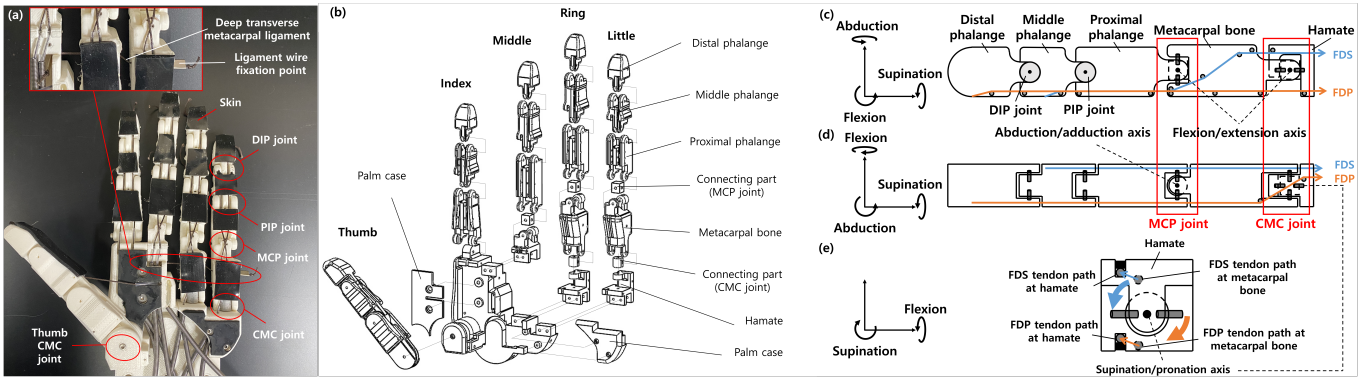

Fig. 3. **Design of the joint structure and tendon path of the proposed prosthetic hand.** (a) The proposed prosthetic hand is composed of the CMC, MCP, PIP and DIP joints, and the deep transverse metacarpal ligaments are connecting the metacarpal bones. (b) The exploded view of the design of the proposed prosthetic hand. (c) Lateral view of the fourth and fifth finger structures. The FDP tendon exerts flexion to all joints and the FDS tendon exerts flexion to DIP, PIP and MCP joints and extension to CMC joint. (d) Top view of the fourth and fifth finger structures. The FDP tendon exerts abduction to the MCP joint and the FDS tendon exerts adduction to the MCP joint. (e) Frontal view of the fourth and fifth CMC joints. The FDP tendon exerts supination to the CMC joint and FDS tendon exerts pronation to the CMC joint.

The arthrokinematics at the CMC joints of the hand produce concavity of the palm, allowing the fingers and the palm to fit around the club. The coupled motion of flexion and supination of CMC joints folds metacarpal bones toward the center of the hand, producing concavity of the palm and wrapping the club diagonally (Figs. 2(a) and 2(b)). In addition, abduction/adduction at metacarpophalangeal (MCP) joints also helps the fingers conform to the club surface, grasped diagonally (Fig. 2(a)) [2].

Another important anatomical structure that enlarges the reach length is the two-rowed structure of the wrist constructed by eight carpal bones (Fig. 2(c)), which allows radio–ulnar deviation. The eight carpal bones construct an arc-shaped proximal row and distal row (Fig. 2(c)); radio–ulnar deviation is produced by rolling and gliding among these arc-shaped rows and the radius/ulnar bones of the forearm. A short pisiform structure of human hand enlarges the ROM of ulnar deviation of the wrist [38], since it forms a small arc radius of the proximal row (Fig. 2(c)) along the ulnar side, allowing more rolling. The increased ROM of ulnar deviation enables the alignment of the forearm with the club. We should also note that the two rowed structure allows the rotational axis to be placed inside the palm, thereby enabling the club to be closely aligned with the forearm with small offset when the wrist is ulnar deviated.

The adjustments of joint stiffness are also important for a stable grasp and efficient swing. The stiffness of human hands could be increased with multiple flexor muscles that contract simultaneously enabling a stable grip. The flexor digitorum profundus (FDP) and flexor digitorum superficialis (FDS) are the main contributors to bend the fingers against resistance or at a high speed motion so that the object could be firmly grasped with the entire hand (Figs. 2(a) and 2(d)) [6]. In particular, the FDS functions more as a reserve muscle, activated when high-power fists or isolated proximal interphalangeal joint (PIP) flexion are needed, while the FDP activates both in high and low powered fists [6].

The change of the effective joint stiffness of the wrist during swinging is important for maximizing the clubhead speed at impact by inducing phase-shifting of joint coordination. A swing is usually generated through two phases: 1) the cocking phase and 2) the swing phase [3]. In the cocking phase, the wrist is radially deviated and pronated, reducing the reach length and initial inertial resistance of swinging (Figs. 1(a) and 1(b)). This allows maximizing the rotational speed of the arm with same level of energy. To retain the wrist posture, the effective stiffness of the wrist remains high at this stage. During the swing phase, the velocity of the club is maximized by aligning it with the arm just before impact (increasing reach length), achieved by releasing (ulnar deviation and supination) the cocked wrist at a certain point (Figs. 1(a) and 1(b)). Instantaneous reduction of effective joint stiffness enables wrist motion at this stage. In other words, the phase-shifting of joint coordination is induced by providing nonlinearity in wrist joint stiffness during the swing.

III. Hand Design

A. Finger joints design based on arthrokinematics

The proposed hand, composed of CMC, MCP, PIP, and DIP joints and bones, has 15 joints, similar to anatomical configuration of human hands (Figs. 3(a) and 3(b)). The joints were designed by adopting arthrokinematics of the human hand.

The prosthetic hand was designed to achieve palm concavity that enables the power squeeze grip (Fig. 2(b)). To produce palm concavity, the CMC joint design replicated the joint arthrokinematics at the fourth and fifth CMC joints. The CMC joint was designed with 2-DOF pin joints enabling flexion and supination motion. The 2-DOF pin joint consists of a metacarpal bone, hamate, and a connecting part, and has a rotating axis about the flexion/extension and supination/pronation of the fourth and fifth metacarpal bones (Figs. 3(c), 3(d) and 3(e)). To prevent excessive flexion in the CMC joints, a deep transverse metacarpal ligament that restrains the flexion ROM in the CMC joints by connecting the palm and the metacarpal bones was mimicked using wires (Figs. 2(a) and 3(a)). Wires used for the deep transverse metacarpal ligaments connected the palm, the fourth metacarpal bone, and the fifth metacarpal bone through holes in each part (Fig. 3(a)). High stiffness synthetic fiber ropes were used for the ligaments

This article has been accepted for publication in a future issue of this journal, but has not been fully edited. Content may change prior to final publication. Citation information: DOI 10.1109/TMECH.2021.3084311, IEEE/ASME Transactions on Mechatronics

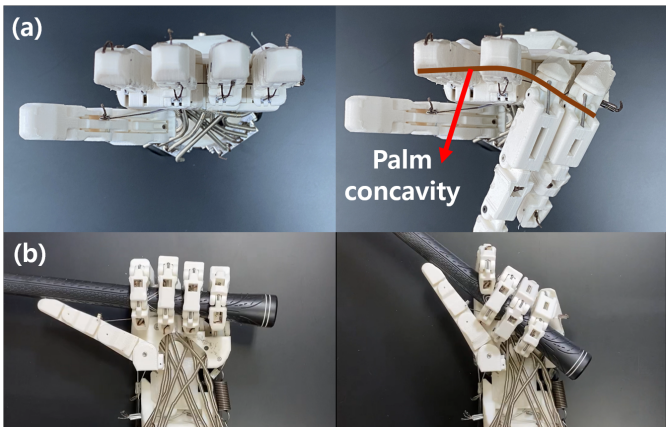

Fig. 4. **Adaptable grasping of the proposed prosthetic hand produced by achieving palm concavity.** (a) Concavity of palm achieved by the designed CMC joints. (b) Adaptable club grasping for various holding angles achieved by the tendon path design of 2-DOF under-actuation.

to limit the flexion ROM in the CMC joints by maintaining the distance between metacarpal bones. The palm concavity produced by the 2-DOF CMC joints and the deep transverse metacarpal ligament is shown in Fig. 4(a).

The tendon path at the CMC joint was designed to produce 2-DOF under-actuation, to allow the fourth and fifth metacarpal bones to adapt to the club. The flexion tendon at the CMC joint (FDP tendon) followed the path, which is shortened when the supination occurs (Figs. 3(c) and 3(e)). The FDP tendon produced tension on the metacarpal bone along both flexion and supination directions so that one motion occurs even when the other motion is blocked. To maintain the position of the metacarpal bone after holding the club, the FDS tendon was routed around the CMC joint to produce 2-DOF under-actuation, consisting of extension and pronation in a similar manner. The fourth and fifth metacarpal bones adapted to the club regardless of the holding angle through the designed tendon path at the CMC joints (Fig. 4(b) and supplementary video).

The MCP joints of the third, fourth, and fifth fingers were designed with a 2-DOF pin joint composed of flexion/extension DOF and abduction/adduction DOF like human hands, to avoid interference between fingers caused by the movements of the fourth and fifth fingers toward the center of the palm. The 2-DOF MCP joint consists of the metacarpal bone, proximal phalange, and a connecting part with a rotating axis about flexion/extension and abduction/adduction (Figs. 3(c) and 3(d)). The tendon was routed to produce 2-DOF under-actuation of the MCP joint, including flexion and abduction. The flexion tendon at the MCP joint (FDP tendon) followed the path that is shortened when abduction occurs (Figs. 3(c) and 3(d)). The FDP tendon exerts tension to the proximal phalange in the directions of flexion and abduction, so that one motion occurs even when the other motion is blocked. The FDS tendon was routed to produce 2-DOF under-actuation, consisting of flexion and adduction, to adjust the degree of abduction/adduction motion while exerting contact force on the club by proximal phalange.

The PIP joints and DIP joints in each finger were designed as a single-DOF pin joint with flexion/extension motion (Fig. 3(c)). The tendon routing at the PIP joints and DIP joints was designed by adopting the tendon routing of the FDP tendon and the FDS tendon of the human hand allowing the fingers to resist external forces (Fig. 2(d)) [39], [40]. The FDP tendon was inserted into the distal phalange, similar to a human hand, and the FDS tendon was inserted into the middle phalange similar to the human hand (Fig. 3(c)). Dyneema, whose diameter was 1 mm, was used for all flexor tendons of the hand. Iron pins and polytetrafluoroethylene (PTFE) sheath were used for pulleys instead of idler pulley for compact design and to decrease friction between the tendon and pulley [36].

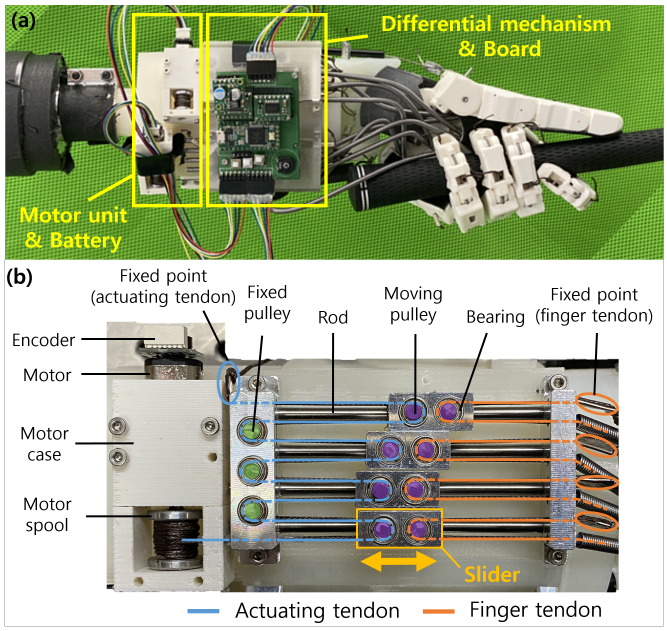

Fig. 5. **Actuation system design of the proposed prosthetic hand.** (a) Proposed prosthetic hand with the overall actuation system. (b) Differential actuation system developed to actuate tendons with a small number of actuations.

The MCP joint of the second finger were designed as a single-DOF pin joint with flexion/extension motion (Fig. 3(c)). The thumb was designed to allow only flexion/extension of the CMC joint focusing on creating and maintaining the club holding angle (Figs. 3(a) and 3(b)).

B. Actuation system design

The actuation system of the proposed hand consists of differential actuation mechanisms to actuate finger tendons with fewer actuators, motor units, and an electronic system to actuate motor units (Fig. 5(a)).

A differential actuation system was implemented to reduce the complexity of actuation by pulling finger tendons with a small number of actuations (Fig. 5 (b)). Differential mechanisms have the advantages of driving fingers with fewer actuators and evenly distributing forces among fingers; therefore, applied in wearable robotic hands and prosthetic hands [37], [38]. In our prosthetic hand, the differential actuation system consists of sliders containing moving pulleys, fixed pulleys, and rods guiding the sliders. When the actuating tendon is pulled (Fig. 5 (b), navy line), all sliders move in a direction that the actuating tendon shortens. When some fingers contact

This article has been accepted for publication in a future issue of this journal, but has not been fully edited. Content may change prior to final publication. Citation information: DOI 10.1109/TMECH.2021.3084311, IEEE/ASME Transactions on Mechatronics

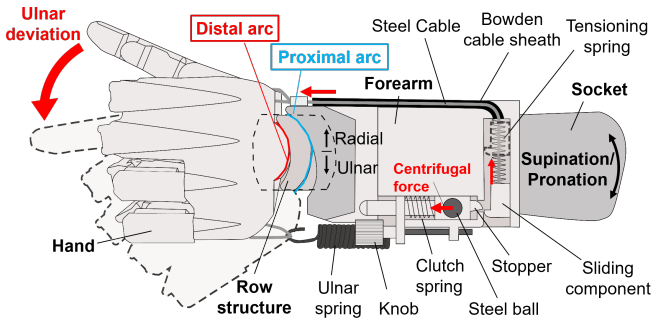

Fig. 6. **Overview of the clutch mechanism and the wrist design.** The wrist ulnar deviates when the sliding component slides along the radial direction. The socket can rotate freely with respect to the wrist structure to embody the DOF of pronation/supination.

with an object, the corresponding sliders are stopped while the moving pulley allows the actuator tendon to pull the other sliders, thereby enabling an adaptable grip. Since two tendons are applied for each finger, a total of nine tendon should be actuated, including one tendon that moves the thumb. We apply one differential actuation system to four FDP tendons and the other differential actuation system to four FDS tendons.

The actuation system applied three motor units actuating the differential mechanism for the FDP tendon, the differential mechanism for the FDS tendon, and the thumb. The motor unit consists of a motor, an encoder, and a motor housing. To maintain the tension exerted to the finger without applying current, micro metal gear motors (6V, HPCB, gear ratio 1000: 1) of Pololu with a stall torque of 11 kg · cm which is non-backdrivable were used. The encoder using a magnetic disc and hall effect sensors was used to stop the motor by detecting when the wire is no longer winding.

Electronic system consisted of micro controller unit (Teensy 3.2 board of PJRC), motor driver carriers to operate the motors, and a battery (7.4V, 1500mAh). The battery operates one motor with maximum efficiency for 3.8 hours was used to the proposed prosthetic hand. The actuation system allows the user to hold the club adaptably in a stable manner by pressing a button on the prosthesis.

IV. Wrist Design

A. Wrist design with a two-rowed arc-shape structure

The two-rowed arc-shaped structure of the carpal bones was implemented with two components that replicated the combined configuration of each carpal bone group (distal and proximal rows). The distal row structure was included in the hand base, and the proximal row was designed as an arc-shaped row structure (Fig. 6). The shape of the radius and ulnar bone (Fig. 2(c)) was also replicated in the forearm structure (Fig. 6). The hand, row structure, and forearm are compressed and assembled with a steel cable routed through guiding holes placed at each component.

The prosthetic hand's rotation axis should be maintained near the capitate of the human hand (Fig. 2(c)) to naturally interact with the contralateral hand. The wrist joint with rolling and gliding maintains the rotational axis of radio-ulnar deviation near the capitate [41]. Otherwise, without gliding, the rotation axis will move along the contact point where rolling occurs.

The wrist joint was designed as a two-rowed structure since it allows increasing the radio-ulnar ROM while maintaining small inter-distance deviation among the hand, row structure, and forearm (Fig. 6) during the motion, which is important to keep the location of the rotational axis at the same place.

The ratio between the radius of the arcs of the two-rowed structure was found to be the most important parameter to maximize the ROM while minimizing the inter-distance deviation. The arc radius ratios were set to 0.55 and 0.7 for the proximal-arc/forearm-arc and hand-arc/distal-arc (Fig. 6), respectively. The proposed wrist structure's rotation axis is located 8 mm proximal from the distal-arc, and the deviation was 7.6 mm similar to human for the full ROM (55°) movement [42]. The asymmetric structure of the proximal row of the human wrist possessing a smaller arc radius along the ulnar side (Fig. 6) was also implemented in the design to allow larger ulnar deviation ROM. The ROMs are 40°and 15°for ulnar deviation and radial deviation, respectively.

The supination/pronation motion of the wrist was also implemented by designing the forearm part so that it could rotate relative to the socket of the prosthesis fixed to the residual limb (Fig. 6). The ROM of supination and pronation is 90° for each direction.

B. Clutch mechanism for nonlinear change of wrist stiffness

A clutch mechanism was implemented to replicate the wrist coordination during the swing, keeping the wrist cocked (high stiffness) at the top of the backswing and releasing (instantaneous stiffness reduction) at a certain point during the downswing (Fig. 6). The clutch mechanism consists of a cable attached to a sliding component (slider), a spring that tensions the cable (tensioning spring), a stopper with a mass, and a spring that pushes the stopper (clutch spring) in the proximal direction of the prosthesis (Fig. 6). The motions of the sliding component and the wrist were coupled by the connection between the hand base and the sliding component with the cable. Upon radial deviation of the wrist, the slider engages the stopper and the wrist becomes fixed (high stiffness). The slider and stopper are disengaged, and the wrist motion is allowed when the external force on the stopper along the distal direction (centrifugal force, gravitational force, and pushing force from the slider) exceeds the force from the clutch spring during the swing (supplementary video). Based on this principle, the clutch provides a nonlinear change to the joint stiffness during the swing. Moreover, to adjust the release timing of the wrist with respect to the swing speed, the adjustment of the pushing force of the stopper spring was achieved by changing the compression amount of the clutch spring with the knob (Fig. 6).

V. Experiments & Results

A. Pressure characteristics of the power squeeze grip

To evaluate the function of the CMC joint of the hand for the power squeeze grip, we compared each pressure value for a human hand, the proposed prosthetic hand that has an

This article has been accepted for publication in a future issue of this journal, but has not been fully edited. Content may change prior to final publication. Citation information: DOI 10.1109/TMECH.2021.3084311, IEEE/ASME Transactions on Mechatronics

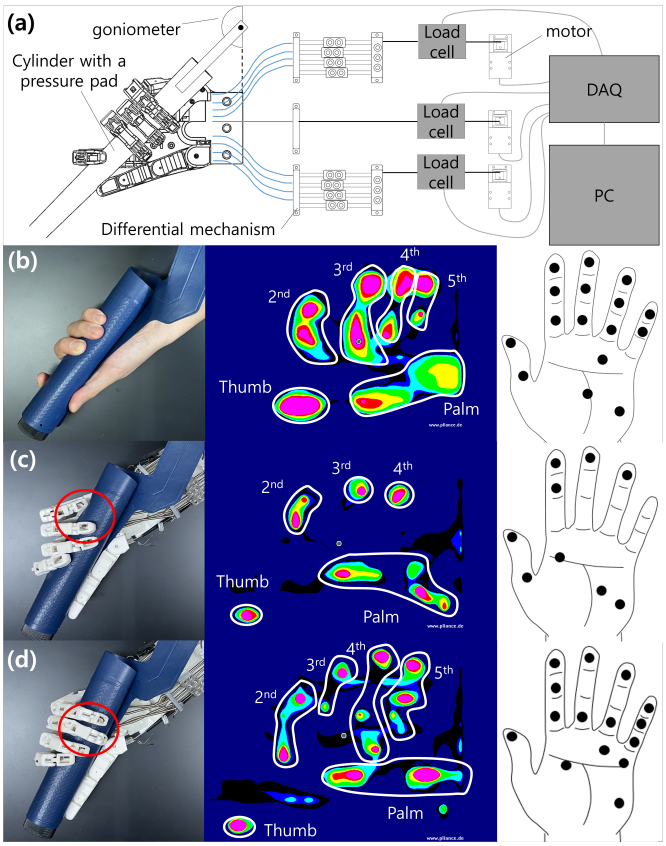

Fig. 7. **Pressure measurement of power squeeze grip.** (a) Pressure measurement experiment setup for the power squeeze grip. (b) Experiment conducted with a human hand to compare prosthetic hands with human hand. (c) Experiment conducted with the prosthetic hand with non-articulated palm. (d) Experiment conducted with the proposed prosthetic hand.

articulated palm composed of CMC joints (experiment group), and a prosthetic hand that has a non-articulated palm (control group), when each hand held the club diagonally. The pressure value was measured by a 35-mm-diameter cylinder wrapped with a pressure pad (pliance® system, novel GmbH, München, Germany), which was gripped by the human hand and the prosthetic hands (Fig. 7 (a)). The prosthetic hands gripped the cylinder diagonally with an angle of 45°between the cylinder and the forearm. The angle and position of the cylinder is kept constant for each experiment using a fixed goniometer in the experimental setup. The tension of the thumb, FDS, and FDP tendons of the prosthetic hands was exerted by same motors applied to the motor unit of the actuation system of the proposed prosthetic hand. To compare the pressure values between prosthetic hands with the articulated palm and the non-articulated palm at equivalent tendon tension, the motor was controlled by sensing each tension with loadcells (5 and 20 kg loadcells, DACELL Ltd., Chungju, South Korea) and DAQ system (NI, Austin, Texas, U.S.). Each prosthetic hand's power squeeze grip was measured five times and the trials of each prosthetic hand were randomized to avoid biased results. For testing with human hands under the same conditions, subjects were told to grip the cylinder with their wrist placed in neutral position and to designate the angle between the cylinder and forearm as 45°. To compare the pressure value of the human hand and that of prosthetic hands on an equivalent pressure scale, the subjects' grasping was measured with various pressure scales, and the results in which the thumb pressure of the subjects (311–341 kPa) was similar to that of prosthetic hands (320 kPa) were used for the analysis. 10 subjects' pressure values of the power squeeze grip were measured.

The pressure values around the hand are shown in Fig. 7 and Table I. The pressure values in the Table I are average values of measured pressure and all values in parentheses are standard deviations of measured values. The prosthetic hand with articulated palm exerted greater pressure on the ulnar side of the hand (ring 596 kPa, little 674 kPa) than the hand with non-articulated palm (ring 253 kPa, little 0 kPa). This result indicates that the fourth and fifth fingers of our hand which adopts arthrokinematics of the CMC joints exert more pressure than those of the hand with non-articulated palm when holding the club diagonally. We compared the normalized pressure value to evaluate the pressure distribution of the power squeeze grip of each hand for equivalent pressure scales by holding cylinders diagonally (Table I). The normalized contact pressure magnitude of the human hand was 4.40 (thumb 1.00, index finger 1.51, middle finger 1.89) and 2.07 (ring finger 1.25, little finger 0.82) on the radial side and the ulnar side, respectively. These contact pressures resisted the impacts of each side during the swing. The pressure magnitude of the prosthetic hand with non-articulated palm was 2.67 (thumb 0.98, index finger 0.91, middle finger 0.78) and 0.78 (ring finger 0.78, little finger 0) on the radial side and the ulnar side, respectively. These results show that the prosthetic hand with non-articulated palm could not exploit the little finger to grasp (Fig. 7(c)), and exerted less pressure on the ulnar side than the human hand. In contrast, the pressure magnitude of the proposed prosthetic hand was 3.52 (thumb 1.00, index finger 1.75, middle finger 0.77) and 3.90 (ring finger 1.83, little finger 2.07) on the radial side and the ulnar side, respectively. In other words, our prosthetic hand with articulated palm exerted more pressure on the ulnar side than the hand with non-articulated palm, while the pressure exerted on the radial side was similar. The pressure exerted by the prosthetic hand with articulated palm on the ulnar side was even greater than that of the human hand. Our CMC joint design achieved power squeeze gripping for the proposed prosthetic hand, which exploited all fingers to grasp diagonally (Fig. 7(d)).

TABLE I
PRESSURE AND NORMALIZED PRESSURE OF POWER SQUEEZE GRIP

		Thumb	Index	Middle	Ring	Little	Palm
Human hand	Pressure (kPa)	325 (24)	497 (128)	544 (233)	406 (193)	252 (160)	1200 (446)
	Normalized Pressure (kPa/kPa)	1.00 (0.00)	1.51 (0.44)	1.89 (0.55)	1.25 (0.53)	0.82 (0.46)	4.06 (1.25)
Prosthetic hand with non-articulated palm	Pressure (kPa)	317 (29)	294 (22)	252 (73)	253 (112)	0 (0)	799 (102)
	Normalized Pressure (kPa/kPa)	0.98 (0.09)	0.91 (0.07)	0.78 (0.22)	0.78 (0.34)	0.00 (0.00)	2.46 (0.31)
Prosthetic hand with articulated palm	Pressure (kPa)	324 (10)	568 (48)	251 (64)	596 (78)	674 (56)	975 (75)
	Normalized Pressure (kPa/kPa)	1.00 (0.03)	1.75 (0.15)	0.77 (0.20)	1.83 (0.24)	2.07 (0.17)	3.00 (0.23)

This article has been accepted for publication in a future issue of this journal, but has not been fully edited. Content may change prior to final publication. Citation information: DOI 10.1109/TMECH.2021.3084311, IEEE/ASME Transactions on Mechatronics

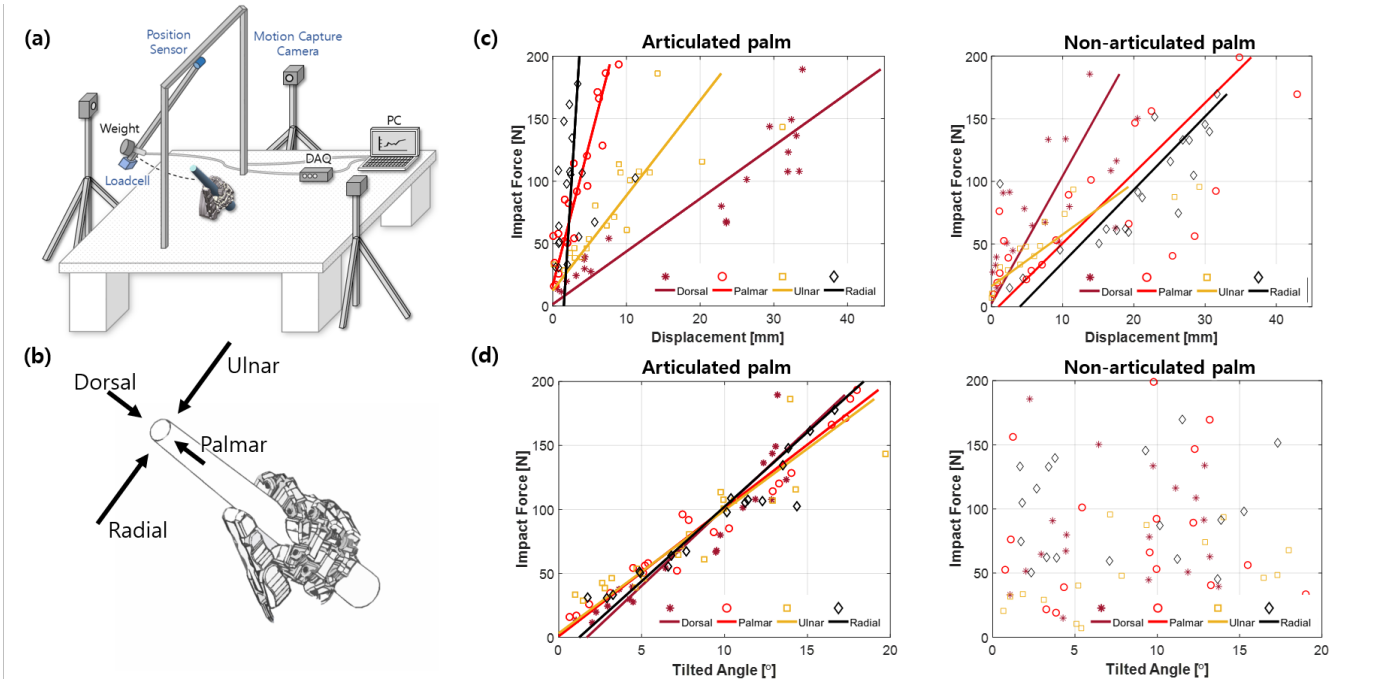

Fig. 8. **Grasp resilience/failure degree for impact test setup and results.** (a) To evaluate the grasp resilience/failure degree of the proposed prosthetic hand to impact and compare it with that of the hand with non-articulated palm, we designed a test setup that exerts impacts on a grasped cylinder using a pendulum. The motion of the cylinder with respect to a prosthetic hand was measured by 3D motion capture cameras. The impact force was measured by a loadcell attached to the tip of the pendulum. (b) The impact was exerted on the grasped cylinder in the dorsal direction, palmar direction, ulnar direction, and radial direction to evaluate the grasp resilience in various directions. (c) Displacements of the cylinder versus impact forces in each hand. (d) Tilted angle of the cylinder versus impact forces in each hand.

B. Grasp quality of power squeeze grip with respect to impact

The grasp quality of the proposed prosthetic hand with the articulated palm was evaluated in terms of grasp resilience and grasp failure degree and compared with those of the prosthetic hand that has non-articulated palm (Fig. 8 and supplementary video). Recently, a benchmark study was conducted to measure potential grasp resilience, the capability of hands to withstand impacts before losing grasp of an object, where the impulsive load of a soft hand was introduced as an index of power grasp quality [10]. Our study evaluated the grasp resilience through the club's displacement versus the impact force and the maximum impact before losing the grasp using the impact test setup (Fig. 8(a)) [10]. The test setup was designed with a pendulum to exert an impact on the hand in various directions. The proposed prosthetic hand with the articulated palm and the hand with the non-articulated palm gripped the cylinder diagonally with an angle of 45° between the cylinder and forearm, and in each impact direction, the pendulum exerted an impact on the cylinder tip. The impact test was conducted in the dorsal, palmar, ulnar, and radial directions (Fig. 8(b) and the impacts were exerted 20 times in each direction. A total of 20 kgf of tension was exerted on each tendon of the thumb, FDS, and FDP. A 20-kg loadcell (DACELL Ltd., Chungju, South Korea) was used to measure the impact force.

The grasp resilience was calculated through the gradient of the linear regression of the experimental results for the club's displacement versus the impact force (Fig. 8(c) and Table II). The gradient of the proposed prosthetic hand with the articulated palm was 4.07, 1.84 and 16.3 times higher than that of the hand with non-articulated palm in the palmar, ulnar, and radial directions respectively. These results indicate that the proposed prosthetic hand can endure higher impact forces than the hand with non-articulated palm in these directions. The gradient of the hand with articulated palm was 2.41 times lower than that of the hand with non-articulated palm in the dorsal direction. This result indicates that the diagonal grasp of the hand with non-articulated palm can endure higher impact force than the proposed prosthetic hand in the dorsal direction. Our prosthetic hand can maintain the grasp on the cylinder for an impact force of approximately 200 N in each direction (dorsal 230 N, palmar 199 N, ulnar 186 N, and radial 223 N).

TABLE II
GRASP RESILIENCE/FAILURE DEGREE OF PROSTHETIC HANDS WITH ARTICULATED/NON-ARTICULATED PALM

		Dorsal	Palmar	Ulnar	Radial
Grasp resilience (N/mm)	Hand with articulated palm	4.23	22.80	7.60	94.80
	Hand with non-articulated palm	10.20	5.60	4.13	5.83
Grasp failure degree (N/°)	Hand with articulated palm	4.828	13.80	35.80	4.58
	Hand with non-articulated palm	321.40	1030.00	90.77	458.70

Our study also estimated grasp failure degree through the variance of the gradients between the origin and each tilted angle of platted data in Fig. 8 (d), because the large variance of the gradient means that the club is tilted regardless of the magnitude of the impact, which means that during impact, the grasp failed. The variance of the gradients between the origin and each tilted angle in each directions was calculated and shown in Table II. The variance of the proposed hand with articulated palm was 66.6, 74.5, 2.54, and 100 times lower than that of the hand with non-articulated palm in the dorsal, palmar, ulnar, and radial directions, respectively. These results indicate that the tilted angle of the club of the hand with non-articulated palm is more varied for each magnitude of impact

This article has been accepted for publication in a future issue of this journal, but has not been fully edited. Content may change prior to final publication. Citation information: DOI 10.1109/TMECH.2021.3084311, IEEE/ASME Transactions on Mechatronics

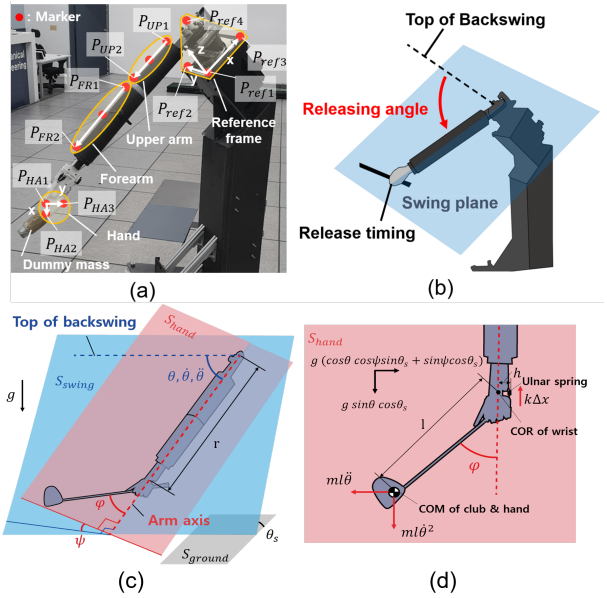

Fig. 9. **Experimental setup for evaluating the clutch performance.** (a) Swing machine and the marker setup. P_{ref1-4} represents the reference frame attached on the swing machine's stationary body. P_{UP1} and P_{UP2} represent the proximal and distal point on the upper arm, respectively. P_{FR1} and P_{FR2} represent the proximal and distal point on the forearm of the swing machine, respectively. P_{HA1}, P_{HA2} and P_{HA3} represents the position and direction of the hand attached on the swing arm, respectively. (b) Design and experimental evaluation of the clutch mechanism. (c-d) Geometrical representation and free body diagram for computing the wrist torque during the swing. S_{swing}, S_{ground}, and S_{hand} represents the swing plane, ground plane, and hand plane (consisting of the arm and club), respectively.

force than that of the proposed hand with articulated palm. The proposed prosthetic hand has less grasp failure degree with respect to impact than the hand with non-articulated palm.

C. Characteristics of wrist stiffness

The characteristic of the wrist joint stiffness was identified from the angular trajectory and estimated external torque of the wrist during the swing generated by the custom-designed swing machine (Fig. 9(a)). The swing was conducted with the same speed while changing the compression of the clutch spring by 0, 2, 4, and 6 mm. The angle of the wrist and the arm was measured by a motion capture system (OptiTrack V120: Trio, NaturalPoint, Inc., Corvallis, OR). Simultaneously, the torque was calculated by considering the inertial, spring-restoring, and gravitational forces.

The torque loading on the wrist joint (τ) could be estimated from the arm angle θ and the wrist angle φ by considering the inertial force due to the arm rotation, restoring force due to the ulnar spring, and torque due to gravity (Fig. 9(b-d)). By assuming the wrist supination (ψ) to be coupled with the arm sharing the same joint angle values ($\psi = \theta$), and the angle between the swing plane and ground (θ_s) is 45°, the wrist torque could be derived as follows.

$$\begin{aligned}\tau &= \tau_{inertial} + \tau_s + \tau_g \\ &= mlr\{\dot{\theta}^2 sin\varphi - \ddot{\theta} cos\theta cos\varphi\} + k\Delta x h \\ &+ mlg\{cos\varphi cos^2\theta sin\theta_s + sin\theta cos\theta_s (cos\varphi + sin\varphi)\}\end{aligned} \quad (1)$$

The wrist stiffness was derived from the slope of the torque plot with respect to the wrist joint angle.

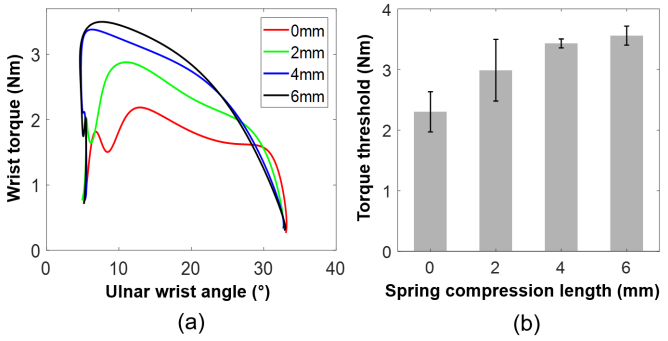

Fig. 10. **Wrist torque with respect to the wrist angle and torque threshold with respect to the spring compression length.** (a) Wrist torque during the swing when max. angular velocity of arm was 100 rpm. (b) Torque threshold for release of the clutch with respect to the clutch spring compression length.

The relationship between the wrist joint angle and the torque during the swing is shown in Fig. 10(a). For all cases, we could observe a nonlinear change in the joint stiffness (slope of plot in Fig. 10(a)) with respect to the wrist joint angle around the point where the maximum torque occurred. We defined this maximum torque as the torque threshold. Before the wrist torque exceeds this threshold, the wrist joint stiffness remains high, restricting the rotation along the ulnar direction; in contrast, when the torque exceeds the threshold, the stiffness dramatically decreases (nonlinear change), allowing the wrist to rotate easily. When the stiffness of the wrist is high, the ulnar deviation angle remains small (cocking), while the ulnar deviation angle dramatically increases (releasing) as the stiffness swiftly reduces. The ulnar wrist angle to wrist torque profile was able to be varied by adjusting the compressed length of the clutch spring. When the compressed length of the clutch increased, the maximum resistive torque increased while the wrist angle that nonlinear stiffness change occurs decreased. With the change of nonlinear stiffness, the prosthetic hand can generate wrist cocking and releasing and the moment of releasing could be adjusted with the compressed length of the clutch spring.

The compressed length of the clutch spring and torque threshold showed positive correlation (Fig. 10(b)). The torque threshold ranged from 2.2 to 3.5 Nm with the adjustment of the compressed length of the spring from 0 up to 6 mm. The results indicate that the torque threshold, and consequently the release timing, could be changed by adjusting the compressed length of the clutch spring.

D. Release timing of the wrist during swing

The release timing of the clutch mechanism of the wrist was experimentally identified with respect to the swing velocity and compression of the spring. The release timing was defined as the moment when the speed of the ulnar deviation of the wrist was maximized, and the timing was represented by the arm angle at that point (releasing angle, Fig. 9(b)).

In many cases of swinging, the releasing angle (Fig. 9(b)) has to maintain a specific value to provide a powerful swing. The performance of our prosthesis in achieving this objective was experimentally evaluated by attaching the wrist mechanism with a clutch to a custom-designed swing machine. For five swing velocity conditions (maximum angular velocities of 70, 80, 90, 100, and 110 rpm), we found the amount of clutch

This article has been accepted for publication in a future issue of this journal, but has not been fully edited. Content may change prior to final publication. Citation information: DOI 10.1109/TMECH.2021.3084311, IEEE/ASME Transactions on Mechatronics

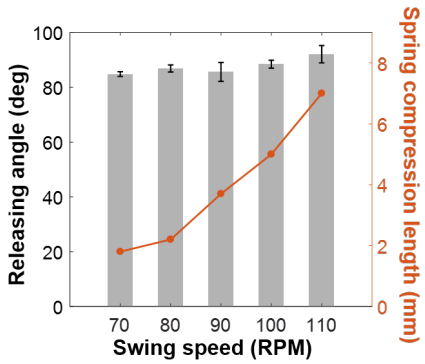

Fig. 11. **Required clutch spring compression length to release at targeted releasing angle for various swing speed conditions.**

spring compression (Fig. 6) that allows the clutch to release at 85°from the top of the backswing (20°before the impact, Fig. 11). Nonlinear positive correlation was found between the swing velocity and clutch spring compression, and the root-mean-squared error of the release angle with the targeted angle was 5.4°. These results indicate that the release angle can be maintained while the swing velocity is changed by adjusting the compression value of the clutch spring, which changes the wrist joint stiffness profile to the ulnar wrist angle (Fig. 10(a)).

E. Golf swing test

Golf swing tests using the swing machine were performed to verify the effects of phase-shift between cocking and releasing during swing (supplementary video). The effect of wrist cocking was evaluated by comparing the swing speed when the wrist was cocked and released and the swing speed when the wrist remained released (ulnar deviated). The maximum angular velocity of the swing machine was set 90 rpm during the test. In the cocking and releasing condition, the clubhead speed just before the impact was 24.8 m/s, an increase of 19.0 % compared to the condition that the wrist was maintained released. This result shows that the phase-shift between cocking and releasing by the wrist clutch mechanism could increase the clubhead speed at impact.

By comparing the golf swing by the prosthetic hand to that of a human subject with 3 years of golf experience (male, 27 yrs), we could notice that the proposed prosthesis could achieve similar wrist deviation angle profile on each golfing phase with the golf swing of the human subject (Fig. 12). Small increase of ulnar deviation was shown in the cocking phase while relatively large increase was shown in the releasing phase.

Golf swings were also performed by non-amputee golfers wearing our hand to evaluate its grasp ability for real swings (Fig. 1, supplementary video). Two golfers performed golf swings using our hand instead of their left hand to hit golf balls. To provide similar physical constraints of amputees, the prosthetic hand was fixed parallel to the forearm and the wrist movement was constrained to prevent the wrist from causing prosthetic hand movements (Fig. 1). The results show that our hand holds the club stably against high-speed swings and impacts.

The experimental protocol was approved by the Institutional Review Board at Korea Advanced Institute of Science and

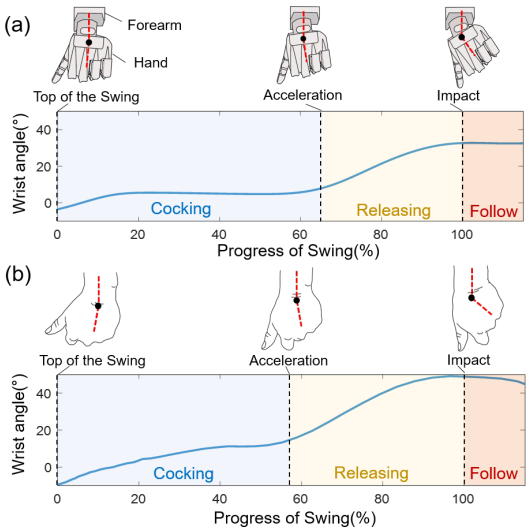

Fig. 12. **Wrist deviation angle during golf swing.** (a) Proposed prosthetic hand, (b) Human subject. Progress of swing is the arm angle normalized to the arm angle deviation during downswing (top of the swing [0%] to impact [100%]).

Technology (KH2019-120), and written informed consent was obtained from each subject prior to participation.

VI. Discussion & Conclusion

In this study, we developed an anthropomorphic prosthetic hand inspired by efficient swing mechanics for sports activities. Our prosthetic hand's diagonal and stable grasp contributes to the efficiency of swinging by aligning the club and forearm to increase the reach length. The wrist mechanism including an inertial clutch also contributes to maximizing the swing speed at impact by modulating the joint stiffness so that the rotational inertia remains low in the early phase of the swing with the wrist cocked (high stiffness condition) and abruptly increases from the change in reach length via wrist ulnar deviation (low stiffness condition) near impact.

The palm concavity achieved by replicating arthrokinematics at the fourth and fifth CMC joints enabled the club to be stably grasped regardless of the holding angle. The palm concavity enabled the diagonally placed club to be wrapped with the fourth and fifth fingers, thereby exerting greater pressure on the club compared to non-articulated palm design. This feature induced higher grasp resilience in the palmar, ulnar, and radial directions (Fig. 8(c) and table II). Particularly, the greatest increase of resilience with the proposed design was shown in radial impacts, as the fourth and fifth fingers of the hand with non-articulated palm could not exert force that resists a radial impact against a club held diagonally. Even though the grasp resilience of the proposed prosthetic hand in the dorsal direction is lower than that of the hand with non-articulated palm, the proposed prosthesis can endure about 20kgf impact in each direction (Fig. 8(c)) and withstand external forces and impacts on the club during 92 rpm swing machine testing. The proposed hand has lower grasp failure degree the the hand with non-articulated palm from the comparison of club's tilted angle shifting for each impact force. The articulated palm allows the fourth and fifth fingers to wrap the club and reduces the grasp failure degree of our prosthetic hand for impact (Fig. 8(d) and table II). This result enables the amputee to exert

impact to a target with the club reliably by swinging. The grasp quality results imply that the concavity of the human hand, which allows the hand to conform to the club, is important for resisting impacts while holding the club diagonally.

In powered prosthetic hand and wrist design, actuators are selected to satisfy predefined task requirements. As many of the upper limb tasks in sports involve high speed and impact, high-powered motors would be required for highly dynamic tasks, resulting in a bulky and heavy design. On the other hand, existing passive prosthetic hands are light and compact, which are good characteristics for simple grasping or holding; thus, the role of the wrist has been as a mechanical interface between forearm and the hand prosthesis. However, in highly dynamic tasks, humans fully utilize the ROM of the wrist in multiple DOFs; therefore, there have been no light and compact prosthetic hands that facilitate highly dynamic tasks. The wrist mechanism proposed herein allows the user to control and maximize swinging speed by using the bio-inspired design of the wrist mechanism instead of using powered actuators for high-speed wrist movement control. Humans maximize swinging speed by the rapid release in the ulnar deviation in most of the swinging tasks, and the speed could be further increased by supination/pronation. The wrist design of our prosthetic hand employs these biomechanical principles to achieve natural and high-speed swinging.

The proposed prosthetic hand can be used for sports activities that require high-load and high-speed swing, and it can contribute to improving the quality of life for amputees by allowing them to engage in sports activities. The designed arthrokinematics of the joints and tendon routing of our prosthetic hand can be also applied to other grasping cases, including ADLs. The palm concavity produced by CMC joints can be applied to anthropomorphic prosthetic/robotic hands for unstructured object grasping by conforming the hand to the shape of objects. The tendon routing inspired by multiple human flexors and the differential actuation system can be applied to prosthetic hands, which need to sustain external loads by holding heavy objects.

Our proposed sports-dedicated prosthetic hand has several limitations to be noted for further study. In this study, only the power squeeze grip with adducted thumb was considered, while many of grasping task are conducted with the thumb abducted. Therefore, future work should also consider the effects of thumb arthrokinematics for the physical activities. There are also several issues to be further considered in the proposed hand system. In the current design, the system does not include sensors. However, as for the future direction, tactile sensors and user intention detection will be important considerations to improve the amputees' sports abilities similar to or even higher than non-amputees' in sports-dedicated prosthesis. For even greater robotic autonomy, the cocking and releasing timing should be automatically adjusted according to the swing speed. One possible solution to achieve this with minimal actuation load would be to place inertial sensors around the socket for measuring the swing speed and to adjust the release timing of the clutch mechanism of the wrist electronically based on the measurements.

ACKNOWLEDGMENT

We thank Prof. Hyun Sik Gong (College of Medicine, Seoul National University) for taking an X-ray of the carpal bone structure during wrist deviation and Jamie Jeong-Ryul Song for working on the figures.

REFERENCES

[1] R. W. Young,"Evolution of the human hand," *J. Anat.*, vol. 202(1), pp. 165–174, 2003.

[2] M. W. Marzke, K. L. Wullstein, and S. F. Viegas, "Evolution of the Power ("Squeeze") Grip and Its Morphological Correlates in Hominids," *Am. J Phys. Anthropol.*, vol. 89, pp. 283–298, 1992.

[3] S. W. Wolfe, J. J. Crisco, C. M. Orr, and M. W. Marzke, "The dart-throwing motion of the wrist," *J. Hand Surg.*, vol. 31A(9), pp. 1429–1437, 2006.

[4] M. W. Marzke and K. L. Wullstein, "Chimpanzee and human grips: A new classification with a focus on evolutionary morphology," *Int. J. Primatol.*, vol. 17(1), pp. 117–139, 1996.

[5] M. M. Skinner, N. B. Stephens, Z. J. Tsegai, A. C. Foote, N. H. Nguyen, T. Gross, D. H. Pahr, J-J. Hublin, and T. L. Kivell, "Response to Comment on "Human-like hand use in Australopithecus africanus"," *Science*, vol. 347, pp. 395–399, 2015.

[6] D. A. Neumann, Kinesiology of the musculoskeletal system: foundations for rehabilitation *Elsevier Health Sciences*, 2013.

[7] M. Bragaru, R. Dekker, J. H. B. Geertzen, and P. U. Dijkstra, "Amputees and Sports," *Sport. Med.*, vol. 41(9), pp. 721–740, 2011.

[8] K. Yazicioglu, M. A. Taskaynatan, U. Guzelkucuk, and I. Tugcu, "Effect of Playing Football (Soccer) on Balance, Strength, and Quality of Life in Unilateral Below-Knee Amputees," *Am. J. Phys. Med. Rehabil.*, vol. 86(10), pp. 800–805, 2007.

[9] P. M. Valliant, I. Bezzubyk, L. Daley, and M. E. Asu, "Psychological Impact of Sport on Disabled Athelets," *Psychol. Rep.*, 56, pp. 923–929, 1985.

[10] F. Negrello, W. Friedl, G. Grioli, M. Garabini, O. Brock, A. Bicchi, M. A. Roa, and M. G. Catalano, "Benchmarking Hand and Grasp Resilience to Dynamic Loads," *IEEE Robot. Autom. Lett.*, vol. 5(2), pp. 1780–1787, 2020.

[11] M. Controzzi, C. Cipriani, B. Jehenne, M. Donati, and M. C. Carrozza, "Bio-Inspired Mechanical Design of a Tendon-Driven Dexterous Prosthetic Hand," in *Proceedings of the Annual International Conference of the IEEE Engineering in Medicine and Biology Safety*, 2010, pp. 499–502.

[12] M. Grebenstein, M. Chalon, W. Friedl, S. Haddadin, T. Wimböck, G. Hirzinger, and R. Siegwart, "The hand of the DLR Hand Arm System: Designed for interaction," *Int. J. Robot. Res.*, vol. 31(13), pp. 1531–1555, 2012.

[13] A. Deshpande, Z. Xu, M. J. Weghe, B. H. Brown, J. Ko, L.Y. Chang, and Y. Matsuoka, "Mechanisms of the Anatomically Correct Testbed Hand," *IEEE/ASME T. Mech.*, vol. 18(1), pp. 238–250, 2013.

[14] C. Melchiorri, G. Palli, G. Berselli, and G. Vassura, "Development of the UB Hand IV: Overview of Design Solutions and Enabling Technologies," *IEEE Robot. Autom. Mag.*, vol. 20(3), pp. 72–81, 2013.

[15] Y.-J. Kim, J. Yoon, and Y.-W. Sim, "Fluid Lubricated Dexterous Finger Mechanism for Human-like Impact Absorbing Capability," *IEEE Robot. Autom. Lett.*, vol. 4(4), pp. 3371–3978, 2019.

[16] N. Kim, S. Yun, and D. Shin, "A Bioinspired Lightweight Wrist for High-DoF Robotic Prosthetic Arms," *IEEE/ASME T. Mech.*, vol. 24(6), pp. 2674-2683, 2019.

[17] J. Vertongen, D. Kamper, G. Smit, and H. Vallery, "Mechanical Aspects of Robot Hands, Active Hand Orthoses and Prostheses: a Comparative Review," *IEEE/ASME T. Mech.*, Early Acess, 2020.

[18] C. Tawk, H. Zhou, Emre Sariyildiz, M. Panhuis, G. M. Spinks, and G. Alici, "Design, Modeling and Control of a 3D Printed Monolithic Soft Robotic Finger with Embedded Pneumatic Sensing Chambers," *IEEE/ASME T. Mech.*, Early Acess, 2020.

[19] G. Figliolini, and M. Ceccarelli, "A novel articulated mechanism mimicking the motion of index fingers," *Robot.*, vol. 20(1), pp. 13–22, 2002.

[20] L. Zollo S. Roccella, E. Guglielmelli, M. C. Carrozza, and P. Dario, "Biomechatronic design and control of an anthropomorphic artificial hand for prosthetic applications," *IEEE/ASME T. Mech.*, vol. 12(4), pp. 418–429, 2007.

[21] Y. Kamikawa and T. Maeno, "Underactuated Five-Finger Prosthetic Hand Inspired by Grasping Force Distribution of Humans," in *Proceedings of the 2008 IEEE/RSJ International Conference on Intelligent Robots and Systems*, 2008, pp. 717–722.

[22] A. Furui, S. Eto, K. Nakagaki, K. Shimada, G. Nakamura, A. Masuda, T. Chin, and T. Tsuji, "A myoelectric prosthetic hand with muscle synergy–based motion determination and impedance model–based biomimetic control," *Sci. Robot.*, vol. 4, eaaw6339, 2019.

[23] B. Massa, S. Roccella, M. C. Carrozza, and P. Dario, "Design and Development of an Underactuated Prosthetic Hand," in *Proceedings of the 2002 IEEE International Conference on Robotics and Automation*, 2002, pp. 3374–3379.

[24] S. A. Dalley, T. E. Wiste, T. J. Withrow, and M. Goldfarb, "Design of a Multifunctional Anthropomorphic Prosthetic Hand with Extrinsic Actuation," *IEEE/ASME T. Mech.*, vol. 14(6), pp. 699–706, 2009.

[25] A. Dollar and R. D. Howe, "The Highly Adaptive SDM Hand: Design and Performance Evaluation," *Int. J. Robot. Res.*, vol. 29(5), pp. 585–597, 2010.

[26] L. U. Odhner, L. P. Jentoft, M. R. Claffee, N. Corson, Y. Tenzer, R. R. Ma, M. Buehler, R. Kohout, R. D. Howe, and A. M. Dollar, "A compliant, underactuated hand for robust manipulation," *Int. J. Robot. Res.*, vol. 33(5), pp. 736–752, 2014.

[27] M. G. Catalano, G. Grioli, E. Farnioli, A. Serio, C. Piazza, and A. Bicchi, "Adaptive synergies for the design and control of the Pisa/IIT SoftHand," *Int. J. Robot. Res.*, vol. 33(5), pp. 768–782, 2014.

[28] B. Radocy, "Upper-Extremity Prosthetics: Considerations and Designs for Sports and Recreation," *Clin. Prosthet. Orthosis*, vol. 11(3), pp. 131–153, 1987.

[29] R. Vinet, Y. Lozac'h, N. Beaudry, and G. Drouin, "Design methodology for a multifunctional hand prosthesis," *J. Rehabil. Res. Dev.*, vol. 32(4), pp. 316–324, 1995.

[30] C. W. Heckathorne, "Upper-limb prosthetics: Components for adult externally powered systems," in *Atlas of limb prosthetics: Surgical, prosthetic, and rehabilitation principles*, Mosby Year Book, 1992.

[31] R. F. Weir, "Design of artificial arms and hands for prosthetic applications," in *Standard handbook of biomedical engineering and design*, McGraw-Hill, 2003.

[32] M. J. Highsmith, S. L. Carey, K. I. Koelsch, C. P. Lusk, and M. E. Maitland, "Design and fabrication of a passive-function, cylindrical grasp terminal device," *Prosthet. Orthotics Int.*, vol. 33(4), pp. 391–398, 2009.

[33] "TRS." TRS prosthetics. Available online at https://www.trsprosthetics.com/ (last accessed June 2, 2020).

[34] C. Pylatiuk, S. Schulz, and L. Doderlein, "Results of an Internet survey of myoelectric prosthetic hand users," *Prosthet. Orthotics Int.*, vol. 31(4), pp. 362–370, 2007.

[35] S.-H. Kim, H. In, J.-R. Song, and K.-J. Cho, "Force characteristics of rolling contact joint for compact structure," In *Proceedings of the 2016 IEEE RAS and EMBS International Conference on Biomedical Robotics and Biomechatronics*, 2016, pp. 1207–1212.

[36] Y. Jung and J. Bae, "Torque Control of a Series Elastic Tendon-sheath Actuation Mechanism," *IEEE/ASME T. Mech.*, Early Acess, 2020.

[37] H. In, B. B. Kang, M. Sin, and K.-J. Cho, "Exo-Glove: A Wearable Robot for the Hand with a Soft Tendon Routing System," *IEEE Robot. Autom. Mag.* vol. 22(1), pp. 97–105, 2015.

[38] D. A. Bennett, S. A. Dalley, D. Truex, and M. Goldfarb, "A Multigrasp Hand Prosthesis for Providing Precision and Conformal Grasps," *IEEE/ASME T. Mech.* vol. 24(6), pp. 2674-2683, 2015.

[39] Dennerlein, J. Tigh, E. Diao, C. D. Mote Jr, and D. M. Rempel. "Tensions of the flexor digitorum superficialis are higher than a current model predicts." *J. Biomech* vol. 31(4) pp. 295-301, 1998.

[40] Kursa, Katarzyna, E. Diao, L. Lattanza, and D. M. Rempel. "In vivo forces generated by finger flexor muscles do not depend on the rate of fingertip loading during an isometric task." *J. Biomech* vol. 38(11) pp. 2288-2293, 2005.

[41] P. A. Houglum and D. B. Bertoti, "Brunnstrom's clinical kinesiology," FA Davis, 2011.

[42] B. Akhbari et al.,"Proximal-distal shift of the center of rotation in a total wrist arthroplasty is more than twice of the healthy wrist,"*J Orthop. Res.*, vol.38(7), pp. 1575-1586, 2020.

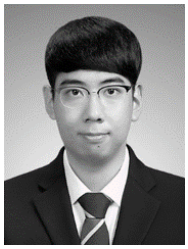

Mun Hyeok Chang received the B.S degree in mechanical engineering from Seoul National University, Seoul, Korea, in 2016, where he is currently working toward the Ph.D. degree with the Biorobotics Laboratory. His current research interests include robotic hand design, actuation mechanism design and control.

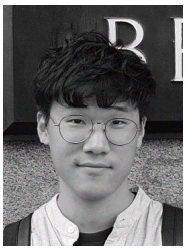

Dong Hyun Kim received the B.S., M.S., and Ph.D. degree in mechanical engineering from Korea Advanced Institute of Science and Technology, Daejeon, Korea, in 2014, 2016, and 2020 respectively. He is currently a postdoctoral researcher at Korea Advanced Institute of Science and Technology, Daejeon, Korea. His research interest includes soft wearable robots, user intension recognition, and control.

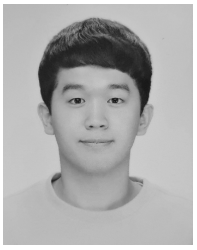

Sang-Hun Kim received the B.S degree in mechanical engineering from Seoul National University, Seoul, Korea, in 2015. where he is currently working toward the Ph.D. degree with the Biorobotics Laboratory. His current research interests include bionic arm and soft wearable robot.

Yechan Lee received the B.S. degree in mechanical engineering from KAIST, Daejeon, Korea, in 2019. He is currently working toward the M.S. degree at the KAIST. His research interests include soft robotics, and rehabilitation engineering.

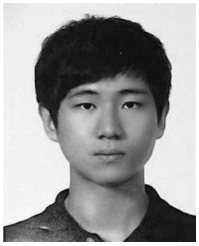

Seongyun Cho received the B.S. and M.S. degree in mechanical engineering from Korea Advanced Institute of Science and Technology, Daejeon, Korea, in 2018 and 2020, respectively. He is currently in a Ph. D. program at Korea Advanced Institute of Science and Technology, Dajeon, Korea. His research interest includes gait rehabilitation, neuromuscular electrical stimulation, and control.

Hyung-Soon Park received the Ph.D. degree in mechanical engineering from KAIST, Daejeon, Korea, in 2004. From 2009 to 2013, he was a staff scientist with Rehabilitation Medicine Department at National Institutes of Health, Bethesda, MD, USA. He is now an Professor in the Mechanical Engineering Department, KAIST, Daejeon, Korea. His current research interest focusses mainly on application of robotics and control technology for effective neuro-rehabilitation, and study of neuromuscular impairments post brain injuries.

Kyu-Jin Cho received the B.S and M.S. degrees from Seoul National University, Seoul, Korea, in 1998 and 2000, respectively, and the Ph.D. degree in mechanical engineering from the Massachusetts Institute of Technology in 2007. He was a Postdoctoral Fellow with Harvard Microrobotics Laboratory until 2008. At present, he is a Professor of mechanical and aerospace engineering, the director of BioRobotics Laboratory at Seoul National University, and the director of Soft Robotic Research Center (SRRC). His research interests include biologically inspired robotics, soft robotics, soft wearable devices, novel mechanisms using smart structures, and rehabilitation/assistive robotics. He has received the 2014 IEEE RAS Early Academic Career Award, 2014 ASME Compliant Mechanism Award, and 2013 KSPE Paik Am Award.